Journal of Image Processing Theory and Applications (2025)
Clausius Scientific Press, Canada

DOI: 10.23977/jipta.2025.080103
ISSN 2560-6239 Vol. 8 Num. 1

New Visual Expression of Movies Based on Matrix Model and Cross-platform Big Data Machine Learning

Shengnan Wang[1,a], Yuanlong Tian[2,b,*]

[1]*Department of Integrated Arts, Silla University, 46958 Busan Metropolitan City, South Korea*
[2]*School of Arts, Weifang University of Science and Technology, Shouguang City, Shandong Province, China*
[a]*w13255364736@163.com*, [b]*19862603283@163.com*
[*]*Corresponding author*

Keywords: Matrix Model, Big Data, Machine Learning, Film New Vision

Abstract: As a unique art, more and more audiences regard visual expression effect as the standard to measure whether a film is of high quality. This study mainly discusses the new visual expression of the film based on matrix model. This paper presents a unified learning system model and programming framework of big data machine based on matrix model. The bridge connecting two views, isolating the upper data analysis programmer and the platform of the bottom big data system is the unified MLDA programming model and interface based on matrix model. Through the unified programming computing model and interface, the upper machine learning algorithm design is decoupled from the distributed and parallel computing system at the bottom, so as to improve the usability of the machine learning system for the data analysis programmer. The movie that will generate the movie clip extracts its keys and extracts the features of those key frames. These unknown samples are put into the proposed semi supervised learning framework with known samples for classification. The classifier will output the label allocation of unknown samples. The last selected key frame is taken to generate a small video clip for each selected key frame for 4 seconds. Finally, these video clips are combined to form a complete movie segment. Our framework not only keeps the highest accuracy of 67.4% in the total average accuracy, but also has a relatively low standard deviation of 0.5. This shows that our framework is not only effective in classification, but also has strong stability and has a positive effect on the performance of new vision of movies.

1. Introduction

With the vigorous development of new media technology, the research on film innovation under the new media environment is increasing. However, the domestic film title research is relatively limited, and the domestic research on film art is mostly limited to film aesthetics, film production technology, film industry and film art education.

Compared with the previous comparative studies, the film fragments are much less. For film fragments, it is usually presented as a small chapter in the film text research. The research on the

application of visual expression of film fragments in the new media environment is of great significance and comparative value.

The compound asynchronous sequence machine (ASM) can be researched through a matrix-based method. Biao believes that the composite ASM is composed of multiple input/state asynchronous machines in a cascaded manner. He obtained the necessary and sufficient conditions of the controller for model matching, and established the algorithm for designing the corresponding controller. Finally, he proposed an example to illustrate the validity of the results obtained. His research lacks data [1]. Chalupa F compares the static modulus determined using uniaxial testing with the dynamic modulus calculated from the elastic wave propagation velocity. To include the effects of damage, the T matrix model has been selected. When he processes the logging data, he only calculates the vertical component of the elasticity tensor. This component is represented by Young's modulus E and Poisson's ratio ν. His research process is too complicated [2]. Kim J M proposed a temperature-dependent behavioral circuit model to predict twisted nematic (TN). He optimized the time constant parameters describing the movement of liquid crystal molecules. He found that the time constant parameter has a linear relationship with the ambient temperature, which allows him to predict the optical response at any given temperature. His research process lacks comparative data [3]. Fedele G proposed a kinematic model to explain the formation of vortices in groups of agents. The main feature of this model is the introduction of two coordinate coupling matrices. These matrices weigh the weight of the attraction term and the reference trajectory of the given target and the interaction term between agents. In addition, he described group aggregation and steady-state properties, and provided numerical simulations to illustrate the results obtained. His research has no practical value [4].

This research proposes a unified big data machine learning system model and programming framework based on the matrix model. The bridge that connects the two views and isolates the upper data analysis programmers and the underlying big data system platform is the proposed unified MLDA programming model and interface based on the matrix model. Through the unified programming computing model and interface, the upper-level machine learning algorithm design is decoupled from the underlying distributed and parallel computing system, thereby improving the usability of the machine learning system for data analysis programmers.

2. New Visual Expression of Film

2.1 Distributed Matrix Multiplication Execution Strategy

Set the input two multiplication matrices and their splitting methods as follows: the number of sub-blocks in matrix A is M, and the number of sub-blocks in matrix B is K. Matrix multiplication $C = AB$ can be written as:

$$C_{i,j} = \sum_k A_{i,k} B_{k,j} \quad i < M \tag{1}$$

For RMM, there is only one shuffle step in the entire execution process [5-6]. In the process of calculating the result matrix C, the input sub-matrix blocks A, k and Be will generate multiple copies[7]. Specifically, there are a total of N copies of sub-blocks of matrix A and M copies of sub-blocks of matrix B. The data volume of shuffle is:

$$shuffle = N_b|A| + M_b|B| \tag{2}$$

CPMM has two shuffle stages, similar to the amount of intermediate process data that can be analyzed, which will not be repeated here[8]. For the concurrency, the concurrency of CPMM sub-block matrix multiplication is K[9]. The concurrency of RMM is:

$$RMM = M_b \times N_b \tag{3}$$

Based on the comprehensive consideration of the advantages of these two execution strategies, this research proposes an optimized execution strategy CRMM (Concurrent Replication-based Matrix Mutiplication)[10-11]. This strategy also includes two shuffle stages, the first shuffle execution process is very similar to RMM, and the second shuffle execution process is similar to CPMM. In this way, CRMM can make a better trade-off between concurrency and the amount of shufle data[12]. In fact, when the dimension k of the input matrix is much smaller than m and n, the implementation of CRMM will be equivalent to RMM; and when the dimension k is much greater than the dimensions m and n, the implementation of CRMM is equivalent to CPMM. In addition, in the case of a large matrix multiplied by a small matrix, in order to avoid full shuffle of the data of the two matrices through the network, this research proposes a Map-side matrix multiplication called Map MM (Map-side Matrix Multiplication)[13-14]. The matrix model is shown in Figure 1.

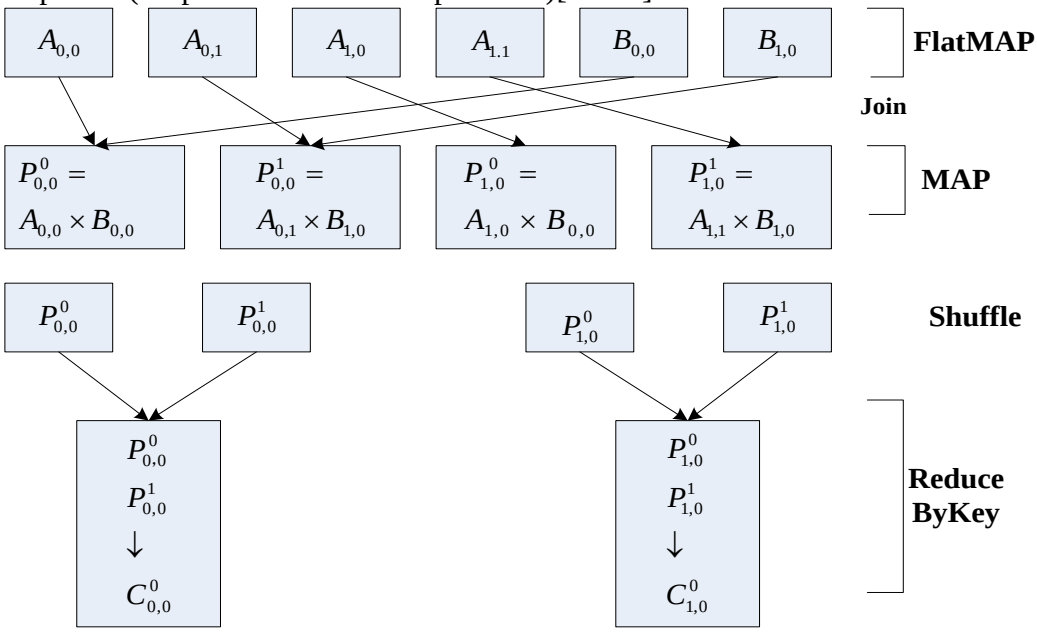

Figure 1. Matrix model

2.2 Machine Learning

Supervised learning qualitatively determines the quality of the classification results while classifying, while unsupervised learning is to cluster the data into different classes and then perform qualitative processing[15]. The results calculated by supervised learning based on the pros and cons of the algorithm itself are unexplainable for its classification reasons, while the results of unsupervised learning will present the clustering reasons, that is, showing the characteristics and consistency of the clustering results[16-17].

Suppose the input of any neuron j in a certain layer is net_j. Its output is y_i. Then there are:

$$net_j = \sum_i w_{ji} y_i \tag{4}$$

$$y_i = f(net_j) \tag{5}$$

$$f(net_j) = \frac{1}{1+e^{-(net_j + h_j)/\theta_0}} \tag{6}$$

w_{ij} is the connection weight between neuron j and neuron i [18]. If j trees are generated in the boosted tree model, the base learner model:

$$y_i = \sum_{j=1}^{J} f_j(x_i),\ f_i \in E(f_i) \tag{7}$$

$$P(t) = \sum_{i=1}^{n} L(y_i, \hat{y}_i) + \sum_{j=1}^{J} E(f_i) \tag{8}$$

f_i is a base classifier in f , and the initial boost tree is f(x) = y . When XG Boost splits a node, it judges whether the node continues to grow according to the gain before and after the split point is added. The gain G:

$$G = \frac{1}{2}\left(\frac{A_L^2}{B_L + \lambda} + \frac{A_R^2}{B_R + \lambda} + \frac{(A_R + A_L)^2}{B_R + B_L + \lambda} \right) - \gamma \tag{9}$$

In the above formula, $\frac{A_L^2}{B_L + \lambda}$ is the score of the left node after the node is split. In addition to the average absolute percentage error MAPE that is commonly used to evaluate the prediction effect, this study also constructs a classification accuracy rate P to assist in the evaluation of the previously established movie box office prediction model[19-20]. The relationship between the average absolute percentage error MAPE and the classification accuracy rate P:

$$MAPE = \frac{1}{n} \sum_{i=1}^{n} |X_i - Y_i| / Y_i * 100\% \tag{10}$$

$$P = \frac{m}{M} * 100\% \tag{11}$$

Where n is the sample size, the predicted value obtained by establishing each supervised learning prediction model training is x_i , and the actual movie box office is y_i .

2.3 SURF Feature Generation

In order to speed up the calculation, SURF uses integral images.

$$I_{\Sigma}(x) = \sum_{i=0}^{i \le x} \sum_{j=0}^{j \le y} I(x, j) \tag{12}$$

The Hessian matrix is defined on the x scale as:

$$H(x, \sigma) = \begin{bmatrix} L_{xx}(x,\sigma) & L_{xy}(x,\sigma) \\ L_{xy}(x,\sigma) & L_{yy}(x,\sigma) \end{bmatrix} \tag{13}$$

Where $L_{xx}(x,\sigma)$ is the second derivative of the image $g(\sigma)$ in the x direction after Gaussian filtering. In order to make the calculation simple, the parameters of the rectangular area are kept very simple, and the solving formula of the characteristic value α is:

$$det(H_{approx}) = D_{xx} D_{yy} - (\omega D_{xy})^2 \tag{14}$$

Among them, ω is an expression used to balance the Hessian determinant. Select the first two edge features as the harrx and harry values, and calculate the angles of the directions of the respective vectors for 109 pixels:

$$angle = \arctan \frac{harry}{harrx} \tag{15}$$

3. Film New Visual Expression Experiment

3.1 Design and Implementation of Matrix Programming Model and Interface

According to the matrix operation required by MLDA, this research provides corresponding matrix operation calculation and programming interface in the programming model and framework. Specifically, the important operating interfaces of BLAS (Basic Linear Algebra Subroutine Library) and LAPACK (Linear Algebra Library) will be implemented and included. According to the different operation objects of the matrix function, this paper designs and provides four levels of large-scale matrix operation interface, which are vector-vector operation, matrix-vector operation and matrix-matrix operation, as well as advanced matrix operation.

1) Level 1: Vector-vector operations, including: vector summation, vector duplication, vector dot product, Euclidean norm of vector, etc.

2) Level 2: Matrix-vector operations, such as matrix-vector multiplication, solving a triangular matrix-vector equation in the form of Ax = b (where A is a triangular matrix, and x and b are vectors).

3) Level 3: Matrix-matrix operations, such as: general matrix addition and subtraction operations, and general matrix multiplication operations, etc.;

4) Level 4: High-level numerical linear algebra calculation interface, mainly including a set of convenient operation interface functions for solving eigenvalues, matrix decomposition (LU, QR, Cholesky and Schur decomposition) problems.

3.2 Unify the Big Data Machine Learning System Model and Programming Framework

A big data machine learning system will involve both the machine learning algorithm design and the underlying big data storage and calculation framework. This research proposes a unified big data machine learning system model and programming framework based on the matrix model. Figure 2 shows the model and programming framework of the unified big data machine learning system.

The upper data analysis programmer view includes the big data MLDA unified programming language and programming development environment layer, the big data MLDA algorithm layer, and the uppermost big data analysis application layer. Based on the unified matrix programming calculation model and interface provided, data analysis programmers can use the R Python programming language and development environment they are familiar with at the unified programming language and programming development environment level to easily and quickly write various MLDA analysis algorithms. Finally complete the development of specific big data analysis applications. The optimized logical execution plan will select a suitable underlying computing platform for execution, thereby forming a physical execution plan: finally, each large-scale matrix operation will be parallelized on the underlying computing platform selected by the physical execution plan.

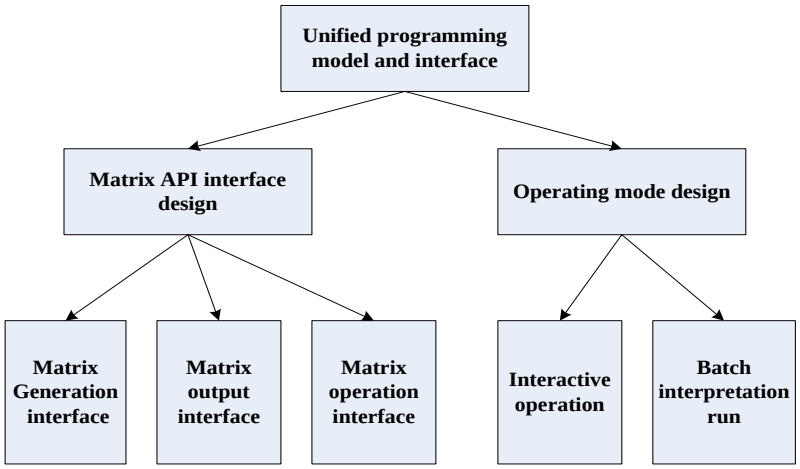

Figure 2. Unified big data machine learning system model and programming framework

The bridge that connects the two views and isolates the upper data analysis programmers and the underlying big data system platform is the proposed unified MLDA programming model and interface based on the matrix model. Through the unified programming computing model and interface, the upper-level machine learning algorithm design is decoupled from the underlying distributed and parallel computing system, thereby improving the usability of the machine learning system for data analysis programmers.

4. New Visual Expressions in Movies

4.1 Semi-Supervised Learning Algorithm

In order to test the effectiveness and robustness of the semi-supervised learning framework proposed by this research, this paper applies the framework to a series of data sets for experiments, this set of data sets includes 10 UCI data sets and 7 SSL data sets. In the research, except for the Constrainedk-means algorithm, other algorithms based on support vector machines all use linear kernels and radial basis function (RBF) kernels. The experiment uses 10 samples as known data. For the SSL data set, it provides a set with 12 records, where each record is the location of 10 known data samples, and we randomly select one of them to define known data; for the UCI data set, we randomly select 10 samples from all data and mark them as known data. Each method was run 20 times, and the results are shown in Figure 3. The basic information of the data set is shown in Table 1.

Table 1. Basic information of the data set

data set	Number of samples	Dimension
Digit1	1500	241
USPS	1500	241
BCI	4000	117
COIL	1500	241
g241c	1500	241
g241n	1500	241
Text	1500	11960
WDC	569	14
Australian	690	33

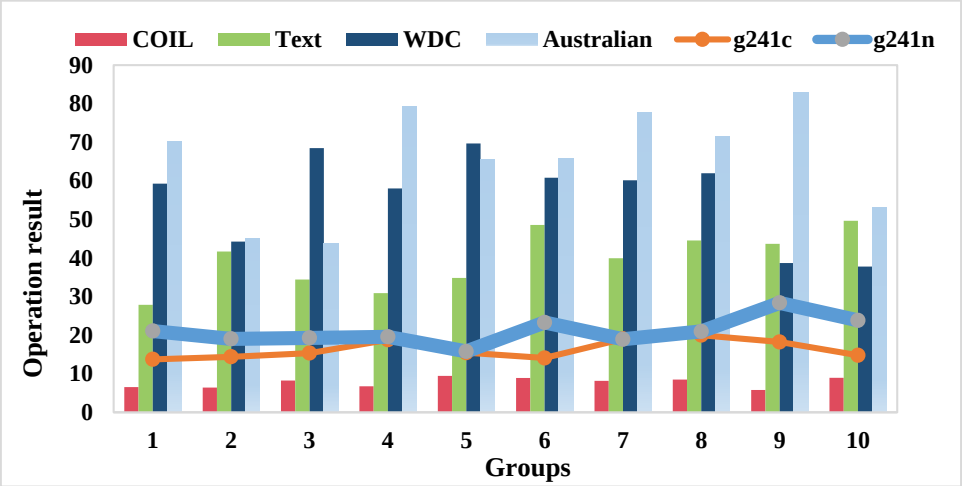

Figure 3. The results of each method being run 20 times

In order to achieve the purpose of comparison, we have compared with multiple algorithms. We use SVM's classification results of the above 17 data sets as a baseline, and other comparison algorithms include Constrainedk-means, SVM, S3VM, S4VM and SSFCM+SVM proposed by Haitao G. Among them, S3VM has two settings. In the first setting, S3VM selects the minimum target value of the low-density classification boundary as the final decision boundary; the second setting is to combine multiple candidate classification boundaries through normalized weights. The performance of our proposed integrated semi-supervised learning framework on the USPS and Australian data sets is not as good as some methods. Through careful observation, we can also find that our framework not only maintains the highest overall average accuracy rate of 67.4%, but also has a relatively low standard deviation of 0.5, which shows that our framework is not only effective in classification problems, but also It also has strong stability. The change trend of the classification accuracy of the german data set is shown in Figure 4.

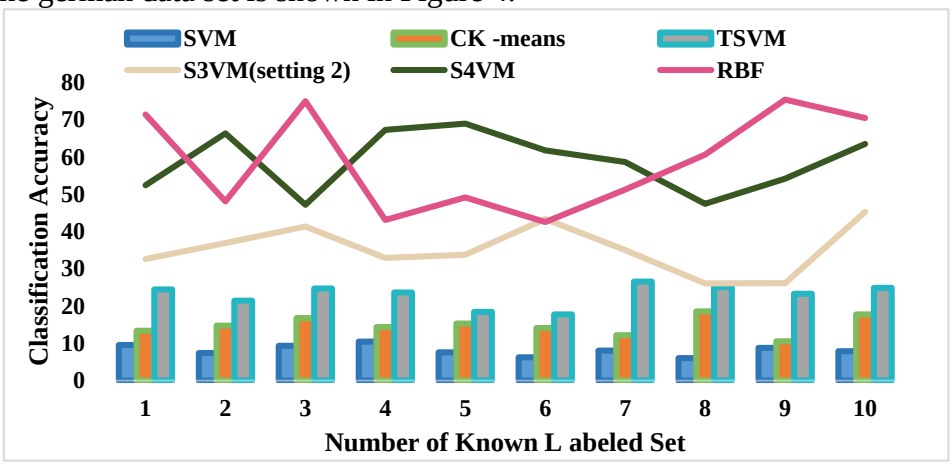

Figure 4. Variation trend of classification accuracy of german data set

Figure 5 shows the change in classification accuracy of the wdbc data set. Intuitively speaking, the semi-supervised learning algorithm should obtain more accurate prediction results when there are more known data. In order to verify this hypothesis, we conducted verification experiments on the wdbc and german two data sets. The number of known samples starts from 10, increases by 10 each time, and is known to 100 known data. You can see the changes in the classification accuracy of the integrated semi-supervised learning framework with different amounts of known data. From

another perspective, these two figures also show that label prediction on unlabeled data has a great influence on the effect of semi-supervised learning. In the semi-supervised learning framework of this research, we try to improve the credibility of label prediction by combining semi-supervised clustering and semi-supervised classification algorithms, in other words, using unknown input data space to obtain predictions from different angles the label should be credible, which provides important information for building a good classifier. However, sometimes for some data set samples, it is difficult for the two semi-supervised learning algorithms to achieve consistency in label prediction.

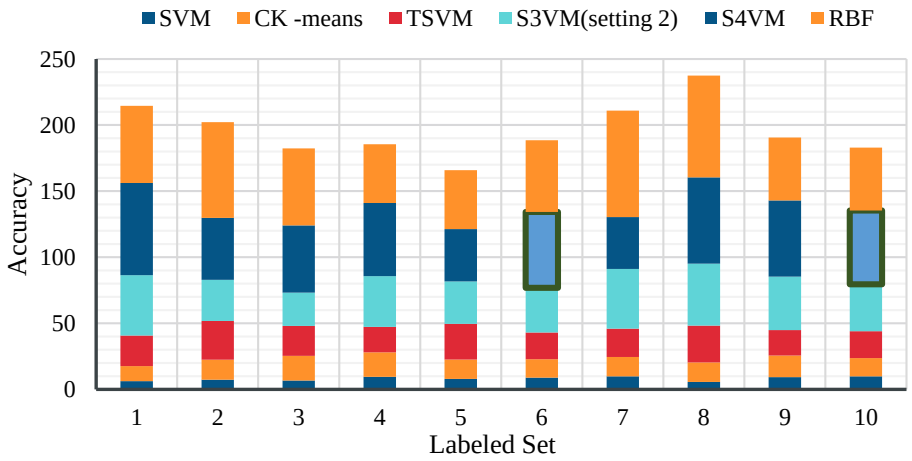

Figure 5. Changes in classification accuracy of the wdbc data set

4.2 Extraction Results of Movie Trailers

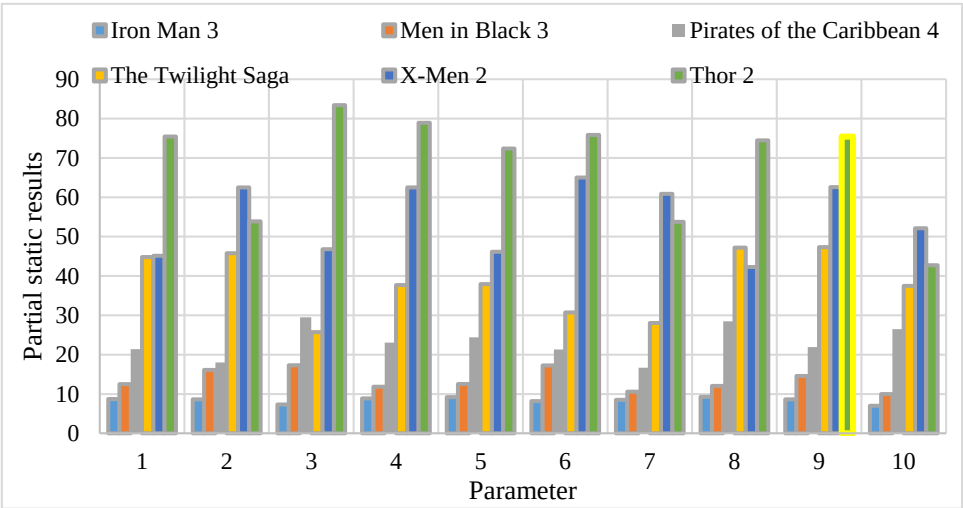

Figure 6. Some static results of our method on the movie

In order to verify the extraction effect of the movie trailers we proposed, we established a dataset of 10 movies. Among these 10 movies, the first 4 movies and their corresponding official trailers are selected as marked data, and the other movies are unmarked data. In order to weigh the time cost and classification accuracy, we set its parameters C1=100 and C2=0.01 in the S4VM algorithm part of the integrated semi-supervised framework. The partial static results of our method on the movie are shown in Figure 6. It can be seen that the trailer content output by our method contains

all the previously mentioned movie trailer elements, namely the protagonist, dialogue, and shocking scenes (this Where is the explosion scene) and the action, that is, the content in the image. It can be seen that our automatically generated trailer and the official manually extracted trailer are more consistent in several trailer elements. In addition, not all movie trailers are those fast-moving or violent scenes, some calmer scenes are also included in the trailer in many cases, and the trailer content we output contains pictures and pictures. The very similar content shows that our method can extract exciting scenes while also extracting quiet and natural scenes that can also promote movies.

Some additional information of the 4 official trailers used as known positive data is shown in Table 2. It is also worth noting that some scenes that appeared in the trailers we generated did not appear in the official trailers. This is because the selection of the content of the movie trailers is greatly affected by human subjective factors, and ours the method is not yet fully in line with some human thoughts, but this does not mean that the scenes we have selected are unattractive. These contents can all be candidates for the content of the trailer. Another point we noticed is that some scenes that appeared in the official trailer were not included in the trailer we generated, indicating that these content is not prominent content for the classifier we use, so the classifier will marked as a negative category.

Table 2. Some additional information for the 4 official trailers used as known positive data

Movie title	Trailer duration (hh: mm: ss)	fps
Prometheus	00: 01: 30	25
The Dark Knight Rise	00: 00: 29	25
Transformers 3	00: 00: 30	25
Inception	00: 00: 52	15

In fact, there is no standard to judge whether a movie trailer is good or bad, and people often rely on their own subjective judgments. Of course, so far there is no unified judgment standard for the results of movie trailers. In this article, we propose a judgment standard that can be compared objectively with numbers and other methods in the future, and can take human subjective factors into account. For movie trailers, we take the official trailer as the completely correct result, calculate the similarity between each frame f in the official trailer and all the frames of the trailer we generated, and find the one that is most similar to f Frame f. If the similarity between the two frames is greater than 80%, the two frames are considered to be a perfect match, and f and f are removed from the trailer frame respectively.

5. Conclusion

In the low-level distributed matrix calculation, we often encounter situations where the distributed row matrix is transformed into a block matrix. In Spark MLIib, the system will use an inefficient method of coordinate conversion, specifically by calculating and transmitting a large number of coordinates. This will bring a lot of additional presentation overhead, and many small objects will also cause a lot of pressure on the system.

This paper proposes a conversion based on the segmentation method, specifically by accurately calculating the data range required by the target block matrix, correspondingly segmenting the source matrix, and then combining the corresponding intermediate data through the aggregation operation to form target matrix block. In this way, a large amount of additional data overhead of coordinates can be reduced, the pressure of disk read and write is reduced, and the overall execution performance is improved.

References

[1] Biao, Wang, Jun-e, et al. Matrix approach to model matching of composite asynchronous sequential machines[J]. IET Control Theory & Applications, 2017, 11(13):2122-2130.

[2] Chalupa F, Vilhelm J, M. Petruálek, et al. Determination of static moduli in fractured rocks by T-matrix model[J]. Acta Montana Slovaca, 2017, 22(1):22-31.

[3] Kim J M, Lee D G, Lee S W. Temperature-Dependent Behavioral Model of Active-Matrix Liquid Crystal Displays for All Types of Liquid Crystals[J]. Journal of Display Technology, 2017, 12(9):881-887.

[4] Fedele G, D'Alfonso L, Bono A. Vortex Formation in a Swarm of Agents With a Coordinates Mixing Matrix-Based Model[J]. IEEE Control Systems Letters, 2019, 4(2):420-425.

[5] Michel B, Polchinski J, Rosenhaus V, et al. Four-point function in the IOP matrix model[J]. Journal of High Energy Physics, 2016, 2016(5):1-25.

[6] Arfib B, De Marsily G. Modeling the salinity of an inland coastal brackish karstic spring with a conduit-matrix model[J]. Water Resources Research, 2017, 40(11):417-427.

[7] Ganesh M, Hawkins S C. Algorithm 975: TMATROM-A T-matrix reduced order model software[J]. ACM Transactions on Mathematical Software, 2017, 44(1):1-18.

[8] Mao S, Zhu M, Yan X, et al. Modeling mechanism of a novel fractional grey model based on matrix analysis[J]. Journal of Systems Engineering & Electronics, 2016, 27(5):1040-1053.

[9] Zotov A V. Calogero–Moser Model and R-Matrix Identities[J]. Theoretical & Mathematical Physics, 2018, 197(3):1755-1770.

[10] Chen A, Zhang M, Zhu Y, et al. Force and Torque Model Utilizing Transfer-Matrix Theory for a Novel Electrodynamic Suspension Reaction Sphere[J]. Iet Electric Power Applications, 2018, 12(1):63-70.

[11] Khvostov A A, Tikhomirov S G, Khaustov I A, et al. Matrix-graph model of the polymer materials destruction process[J]. Proceedings of the Voronezh State University of Engineering Technologies, 2018, 80(3):50-55.

[12] Zhang S, He Z, Li J, et al. A Generalized Covariance Matrix Taper Model for KA-STAP in Knowledge-Aided Adaptive Radar[J]. Ice Transactions on Fundamentals of Electronics Communications & Computer ences, 2016, 99(6):1163-1170.

[13] Tao L, Liu S, Fang Z, et al. Matrix representation model and its solution of GERT network[J]. Systems Engineering and Electronics, 2017, 39(6):1292-1297.

[14] Chen H, Guansheng L, Tao T, et al. A New Approach of Constraints Establishment and Optimization for Matrix Tolerance Model[J]. Journal of Mechanical Engineering, 2016, 52(1):123-129.

[15] Yin S Y, Chen L, Pan M, et al. A Mathematically-Tuning Model of Multicolor and White Light Upconversion in Lanthanide-Doped ZrO 2 Macroporous Matrix[J]. Chemistryselect, 2016, 1(12):3136-3143.

[16] Szollosi A, Baranyi P. Influence of the Tensor Product Model Representation Of QLPV Models on The Feasibility of Linear Matrix Inequality[J]. Asian Journal of Control, 2016, 18(4):1328-1342.

[17] Gervois A. Matrix elements statistics in the shell model[J]. Physics Letters B, 2016, 26(7):413-417.

[18] Gulbudak O, Santi E. FPGA-Based Model Predictive Controller for Direct Matrix Converter[J]. IEEE Transactions on Industrial Electronics, 2016, 63(7):4560-4570.

[19] Agarwal A, Amjad M J, Shah D, et al. Model Agnostic Time Series Analysis via Matrix Estimation[J]. ACM SIGMETRICS Performance Evaluation Review, 2019, 47(1):85-86.

[20] Xia Y, Chen Y, Song Y, et al. An Efficient Phase Domain Synchronous Machine Model With Constant Equivalent Admittance Matrix[J]. IEEE Transactions on Power Delivery, 2019, 34(3):929-940.